Journal of Power Sources 200 (2012) 29–33

Contents lists available at SciVerse ScienceDirect

Journal of Power Sources

journal homepage: www.elsevier.com/locate/jpowsour

Short communication

Enhanced electrochemical performance of $BaZr_{0.1}Ce_{0.7}Y_{0.1}Yb_{0.1}O_{3-\delta}$ electrodes for hydrogen and methane oxidation in solid oxide fuel cells by Pd or $Cu_{0.5}Pd_{0.5}$ impregnation

Jiang-Tao Zhang[a], Feng-Li Liang[b], Bo Chi[a,*], Jian Pu[a], Li Jian[a]

[a] State Key Laboratory of Materials Processing and Die and Mould Technology, School of Materials Science and Engineering, Huazhong University of Science and Technology, Wuhan, Hubei 430074, China
[b] School of Chemical Engineering, The University of Queensland, Brisbane, QLD 4072, Australia

ARTICLE INFO

Article history:
Received 16 August 2011
Received in revised form 21 October 2011
Accepted 22 October 2011
Available online 25 October 2011

Keywords:
Solid oxide fuel cell
$BaZr_{0.1}Ce_{0.7}Y_{0.1}Yb_{0.1}O_{3-\delta}$ anode
Pd impregnation
Hydrogen oxidation
Methane

ABSTRACT

The anode material $BaZr_{0.1}Ce_{0.7}Y_{0.1}Yb_{0.1}O_{3-\delta}$ (BZCYYb) for solid oxide fuel cells (SOFCs) is prepared by solid state reaction method and its chemical compatibility with Y_2O_3 stabilized ZrO_2 (YSZ) is evaluated. The electrochemical performance of the pure and Pd- and $Cu_{0.5}Pd_{0.5}$-impreganated BZCYYb electrodes is characterized in the temperature range between 650 and 750 °C by AC impedance spectroscopy in H_2 and/or CH_4 atmospheres, respectively, under the condition of open circuit. It is confirmed that the BZCYYb is chemically compatible with the YSZ at temperatures below 1000 °C. The polarization resistance of the BZCYYb anode in H_2 is decreased from 2.08 to 0.51 Ω cm^2 as the measuring temperature increases from 650 to 750 °C with an activation energy of 117 kJ mol^{-1}. With Pd- or $Cu_{0.5}Pd_{0.5}$-impregnation, the polarization resistance of the BZCYYb electrode in H_2 is reduced significantly to approximately 0.40 Ω cm^2 at 650 °C and 0.12 Ω cm^2 at 750 °C. With dry CH_4 as the fuel, the polarization resistance of the Pd- and $Cu_{0.5}Pd_{0.5}$-impregnated BZCYYb anodes is obviously increased below 1.00 Ω cm^2 at 650 °C and 0.22 Ω cm^2 at 750 °C. Both Pd and $Cu_{0.5}Pd_{0.5}$ impregnations are equivalently effective in enhancing the electrochemical performance of the BZCYYb anode.

1. Introduction

Solid oxide fuel cells (SOFCs) can utilize a wide variety of hydrocarbon fuels, which makes it tremendous attractive as a promising technology for generation of electrical energy [1]. The conventional anode consisting of Ni and Y_2O_3 stabilized ZrO_2 (YSZ) for the SOFCs has demonstrated excellent performance when hydrogen is used as the fuel, but it is susceptible to carbon deposition (coking) and deactivation (poisoning) by contaminants commonly encountered in readily available fuels [2]. Substantial effort has been devoted to the development of new anode materials and novel electrode structures to solve these problems [3,4]. Various anode catalysts, including ceria-based cermets [5,6], Sr-doped $LaCr_{0.5}Mn_{0.5}O_{3-\delta}$ (LSCM) [7,8], (La, Ca)(Cr, Mn)O_3(LCCM) [9], $Sr_2MgMoO_{6-\delta}$-based double perovskites [10], were reported to be more effective in preventing carbon formation than the conventional Ni-base anodes. Unfortunately, the power density of the SOFCs using these oxide anodes is somewhat low due to their insufficient conductivity or low activity towards hydrocarbon oxidation. Metal catalysts added to the ceramic anodes can facilitate reforming reactions that generate H_2 and CO from hydrocarbons at their operating temperatures (650–750 °C) and can improve the performance of the cell.

$BaZr_{0.1}Ce_{0.7}Y_{0.2}O_{3-\delta}$ (BZCY) [11], which was previously used as a SOFC electrolyte, has attracted a great deal of attention due to its excellent chemical stability at low operating temperatures. However, the conductivity and the electrocatalytic activity of the BZCY have limited its application as an anode material by poor electrochemical performance. To improve the conductivity and electrocatalytic activity of the BZCY, transition metal elements have been introduced into the Y-site. Recently, a chemically stable perovskite-type material, $BaZr_{0.1}Ce_{0.7}Y_{0.1}Yb_{0.1}O_{3-\delta}$ (BZCYYb) [12], is reported for the anode of the SOFCs. It has demonstrated adequate electrochemical stability over a wide range of conditions relevant to SOFC operation, is very effective for in situ reformation of hydrocarbons, and is helpful for inhibiting carbon deposition while hydrocarbon fuels are used.

Wet impregnation has been confirmed to be an effective method to fabricate nano-structured electrodes and enhance electrode electrochemical performance [13,14]. It has been used for the development of the cathodes [15–19] and anodes [20]. And electrode performance can be further promoted by incorporating ionic or electronic conducting phase, such as Gd-doped CeO_2 (GDC) [21]

* Corresponding author. Tel.: +86 27 87558142; fax: +86 27 87558142.
E-mail address: chibo@hust.edu.cn (B. Chi).

0378-7753/$ – see front matter © 2011 Elsevier B.V. All rights reserved.
doi:10.1016/j.jpowsour.2011.10.082

or Pd [22,23] for the cathodes and Cu or Cu–Pd for anodes [20,24]. In the present study, Pd- and $Cu_{0.5}Pd_{0.5}$-impregnated BZCYYb anodes have been evaluated electrochemically, in comparison with the pure BZCYYb anode, with both H_2 and CH_4 as the fuel in the temperature range of 650–750 °C.

2. Experimental

The anode material BZCYYb was prepared by the conventional solid state reaction method [25]. Stoichiometric amount of high-purity barium carbonate, zirconium oxide, cerium oxide, yttrium oxide and ytterbium oxide powders (Sinopharm Chemical Reagent Co., Ltd.) were mixed by ball-milling in ethanol for 48 h, followed by drying in an oven and calcination at 1100 °C in air for 10 h. The calcinated powder was ball milled again, followed by another calcination at 1150 °C in air for 10 h.

The formed phase in the calcinated powder was identified by X-ray diffraction (XRD) using a Phillips X'Pert Pro diffractometer with Cu Kα radiation. The diffraction patterns were registered over a 2θ range between 20° and 80°.The chemical compatibility between the prepared BZCYYb powder and the YSZ (TZ8Y, Tosoh, Japan) electrolyte was studied by firing pressed pellets of BZCYYb/YSZ mixture of 1:1 weight ratio at temperatures of 800, 900, 1000 and 1100 °C in air for 10 h, followed by XRD phase analysis.

The well-sintered YSZ electrolyte pellets (relative density >98%) was prepared by pressing the YSZ powder at a pressure of ~200 MPa and sintering at 1500 °C for 4 h. In order to fabricate the electrode, the BZCYYb powder was mixed with terpineol, ethyl cellulose and proper amount of rice starch to form slurry, which was then screen printed on the sintered YSZ pellets. The BZCYYb/YSZ bilayer was sintered at 1000 °C in air for 2 h to form a porous BZCYYb electrode on the electrolyte. The thickness of the sintered electrode was 10 μm and the effective electrode area was 0.5 cm^2 (0.8 cm in diameter). Nano-sized Pd and $Cu_{0.5}Pd_{0.5}$ alloy particles were also introduced into the porous BZCYYb electrode, respectively, by impregnation of the BZCYYb scaffold with aqueous solutions containing 15 weight percent of HCl and desired amount of $PdCl_2$ and/or $CuCl_2$, followed by heating at 300 °C for 1 h. The impregnation-heat treatment cycle was carried out repeatedly in order to obtain a proper loading of Pd or $Cu_{0.5}Pd_{0.5}$. After reduction in 95% N_2 + 5% H_2 atmosphere at 800 °C for 5 h, the weight percentage of the impregnated catalyst in the BZCYYb scaffold was around 10 wt.%. High temperature silver paste (Sino-Platinum Co., Ltd.) was painted on the top of the BZCYYb electrode as the current collector and on the opposite side of the electrolyte disk as the counter and reference electrodes. The distance between the ring-shaped reference and circular-shaped counter electrodes was 4 mm. Such prepared cells were fired at 850 °C for 2 h.

The three-electrode configuration was used for the electrochemical measurement of the cells with dry H_2 or CH_4 as the fuel and stagnant air as the oxidant. Electrochemical impedance spectra of the cells were obtained in a frequency range of 0.01 Hz to 1 MHz with a signal amplitude of 10 mV at temperatures between 650 and 750 °C using an impedance gain/phase analyzer (Solartron1260) and an electrochemical interface analyzer (Solartron1287) at open circuit. A scanning electron microscopy (SEM, Quanta 200, FEI Corporation, Holland) was employed to examine the cross-sectional morphology of the cells.

3. Results and discussion

In comparison with the JCPDS file 01-089-2485 for cubic perovskite $BaCe_{0.7}Zr_{0.3}O_3$, the XRD pattern of the as-prepared BZCYYb powder is shown in Fig. 1. This pattern is identical to that of the $BaZr_{0.1}Ce_{0.7}Y_{0.1}Yb_{0.1}O_{3-\delta}$ reported by Ding and Xue [26]. The

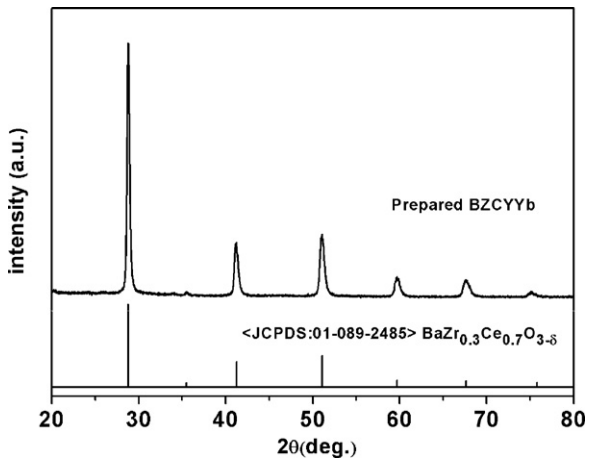

Fig. 1. The X-ray diffraction pattern of the prepared BZCYYb in comparison with JCPDS file 01-089-2485 for cubic perovskite $Ba(Ce_{0.7}Zr_{0.3})O_3$, showing a cubic perovskite structure with a lattice parameter of 0.434 nm.

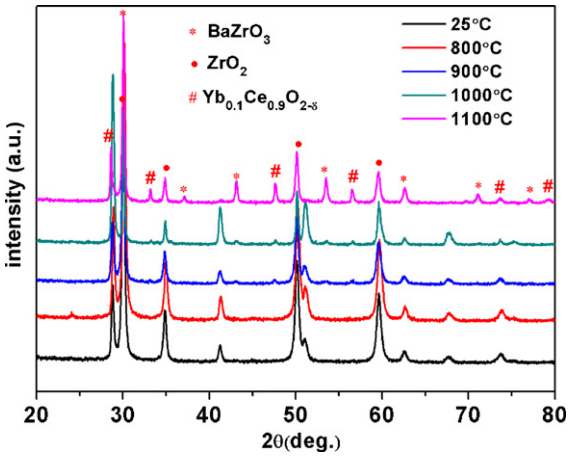

Fig. 2. The X-ray diffraction patterns of a mixture consisting of the BZCYYb and YSZ powders at various temperatures, indicating that the BZCYYb is chemically compatible with the YSZ at temperatures below 1000 °C.

comparison confirms that the prepared BZCYYb is a pure phase with the cubic perovskite structure. Fig. 2 demonstrates the XRD diffraction patterns of the mixed BZCYYb/YSZ powders fired at various temperatures between 800 and 1100 °C in air for 10 h, which suggests that there were no XRD evidence of chemical reactions between the YSZ and the BZCYYb at temperatures below 1000 °C. However, extra phases were formed as the calcination temperature was increased to 1100 °C; some minor peaks corresponding to $Yb_{0.1}Ce_{0.9}O_{2-\delta}$ and $BaZrO_3$ were seen in the XRD spectrum, indicating solid state reaction between the YSZ and the BZCYYb.

By using the above described screen-printing and sintering processes, a layer of uniform and porous BZCYYb anode, as shown in Fig. 3a, was fabricated on the dense and crack free YSZ electrolyte with a well adhered interface. The porosity of the BZCYYb anode was about 37%, which was sufficient for fuel gas diffusion in the pores and oxygen ions/electrons transportation inside the BZCYYb scaffold. With 10 wt.% impregnated Pd or $Cu_{0.5}Pd_{0.5}$, discrete catalyst particles were deposited on the surface of the BZCYYb backbone. The microstructure of the impregnated anode is shown in Fig. 3b and c Fig. 3 for Pd and $Cu_{0.5}Pd_{0.5}$ impregnations, respectively. After impregnation, the porosity of the anodes was somewhat reduced.

Fig. 4 a displays the impedance spectra of the prepared cells with the BZCYYb anode measured under the condition of open circuit in

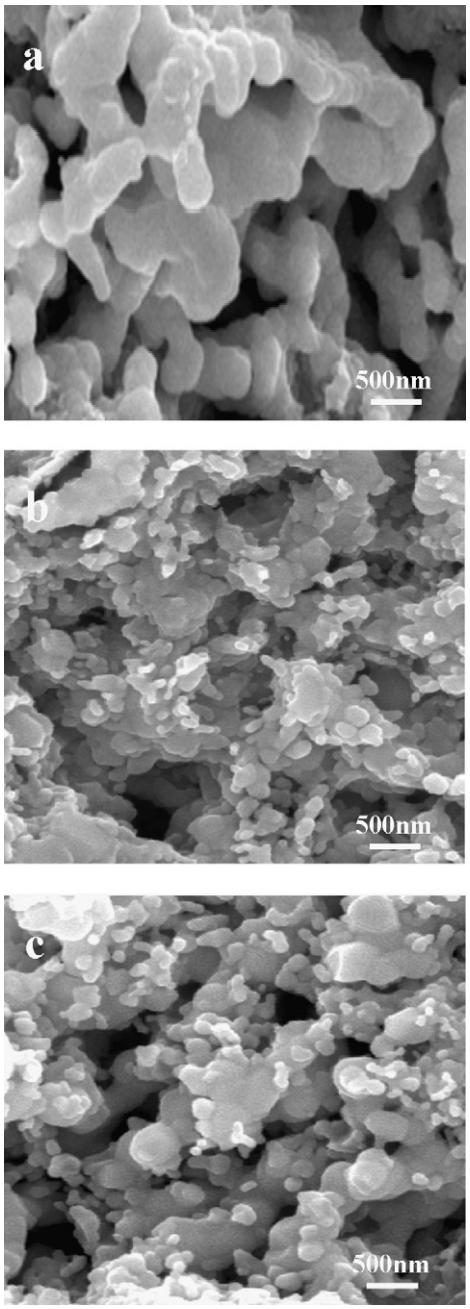

Fig. 3. SEM microstructures of the prepared (a) pure, (b) Pd-impregnated and (c) $Cu_{0.5}Pd_{0.5}$-impregnated BZCYYb anodes.

dry H_2 at different temperatures from 650 to 750 °C. The value at the low frequency intercept with the real axis represents the total cell resistance (R_t); and the value of the high frequency intercept with the real axis represents the ohmic resistance (R_o) of the cell, including the ohmic resistances contributed by the testing leads, electrolyte and electrode. The polarization resistance of the anode R_P, which is not ohmic in nature, is the difference between R_t and R_o. The purpose of the present study is on the electrochemical performance of the anode; and hence only the polarization resistance is of interest hereafter. Fig. 4b shows the R_P as a function of the measuring temperature, which obeys the well-accepted relation [19,27] that

$$R_P = R_P^0 \exp\left(\frac{Q}{RT}\right) \quad (1)$$

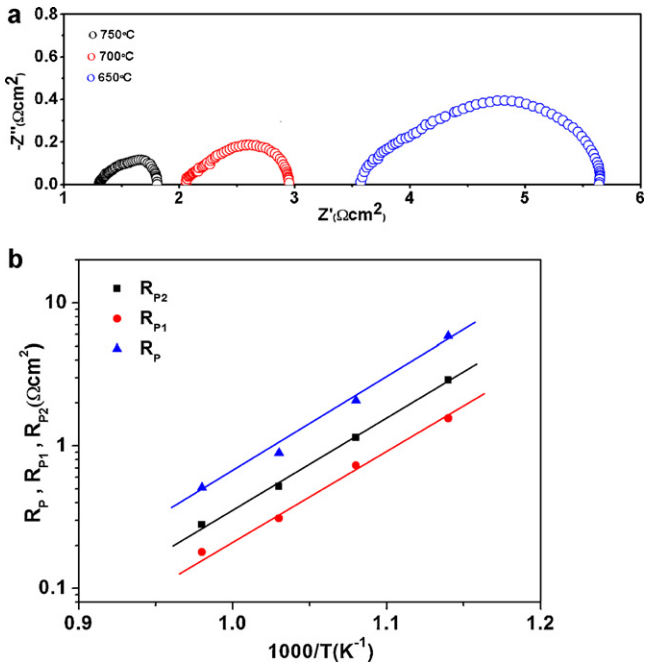

Fig. 4. The electrochemical performance of the prepared pure BZCYYb anode: (a) AC impedance spectra measured at various temperatures between 650 °C and 750 °C under the condition of open circuit; (b) the overall electrode polarization resistance R_P and the deconvoluted polarization resistances R_{p1} and R_{p2} as a function of temperature.

where R_P^0 is a pre-exponential constant and Q the activation energy. As expected, increasing the measurement temperature resulted in a significant reduction in the R_P, typically from 2.08 Ω cm^2 at 650 °C to 0.51 Ω cm^2 at 750 °C with an activation energy of 117 kJ mol^{-1} for hydrogen oxidation in the temperature range. These values of the R_P are lower than those obtained from cells with LCCM/GDC (1.01 Ω cm^2 at 750 °C [9]), LCCM/YSZ(1.4 Ω cm^2 at 900 °C [28]) and LSCM/YSZ(2.1 Ω cm^{2}at 900 °C [28]) composite anodes, which is most likely related to the high catalytic activity and ionic conductivity of the BZCYYb phase below 750 °C as compared to the GDC or LCCM phase in the composites [12].

Conventionally, the polarization arc can be deconvoluted into the high-frequency and low-frequency arcs by an equivalent circuit with a configuration of $(R_{p1} - CPE_1)$ $(R_{p2} - CPE_2)$ as shown in Fig. 5. In the equivalent circuit, the CPE_1 and CPE_2 are the constant phase elements, and the R_{p1} and R_{p2} are the resistances associated with the high- and low-frequency arcs, respectively. It is considered that the high-frequency arc is the characterization associated with the charge-transfer process occurring at the electrode/electrolyte interfaces and the electron-transfer process accompanying with the fuel oxidation reaction; and the low-frequency arc is considered as the convoluted contributions of the adsorption and diffusion of the fuel gas at the gas/anode interface and the surface diffusion of intermediate species [7,19]. The temperature dependence of the R_{p1} and R_{p2} are also shown in Fig. 4b. For comparison the

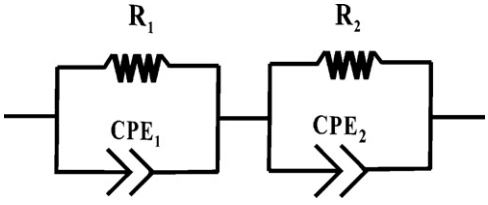

Fig. 5. The electrical circuit used to fit the AC impedance spectra of the prepared pure, Pd-impregnated and $Cu_{0.5}Pd_{0.5}$-impregnated BZCYYb electrodes.

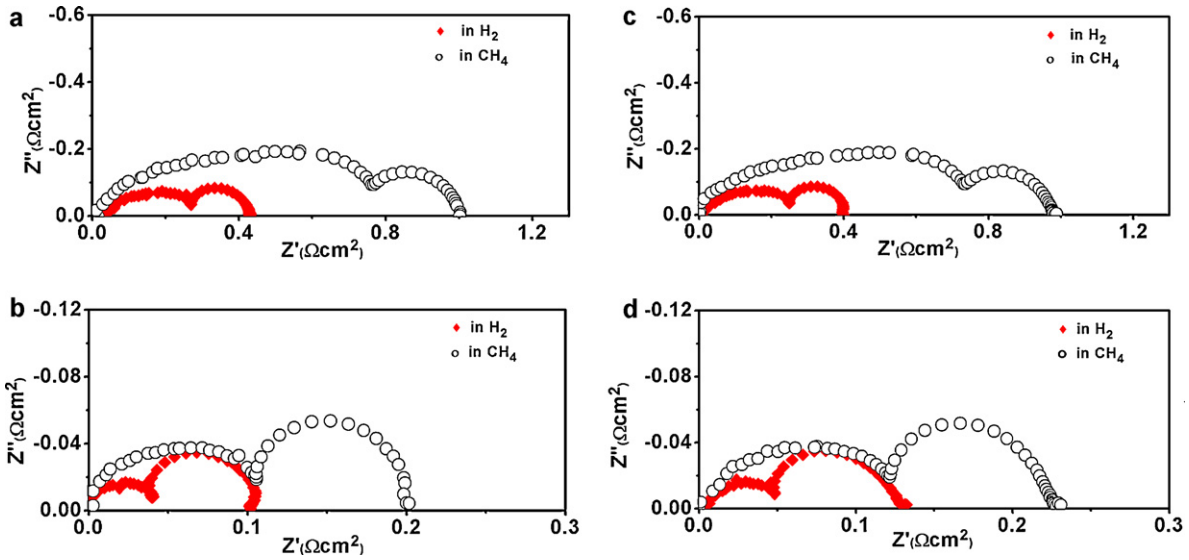

Fig. 6. Open circuit AC impedance spectra of the prepared impregnated BZCYYb electrodes measured in H_2 and CH_4 at various temperatures: (a) and (b) Pd-impregnated at 650 °C and 750 °C; (c) and (d) $Cu_{0.5}Pd_{0.5}$-impregnated at 650 °C and 750 °C.

Table 1
The values of polarization resistances (Ω cm²) of the prepared electrodes in H_2 and CH_4 at various temperatures.

Anode	Temperature (°C)	R_P	R_{p1}	R_{p2}
BZCYYb in H_2	650	2.08	0.39	1.80
	700	0.89	0.36	0.59
	750	0.51	0.29	0.22
BZCYYb + Pd in H_2	650	0.40	0.25	0.14
	750	0.12	0.04	0.08
BZCYYb + Pd in CH_4	650	0.98	0.92	0.12
	750	0.20	0.12	0.10
BZCYYb + $Cu_{0.5}Pd_{0.5}$ in H_2	650	0.39	0.26	0.14
	750	0.12	0.04	0.08
BZCYYb + $Cu_{0.5}Pd_{0.5}$ in CH_4	650	0.99	0.91	0.11
	750	0.22	0.11	0.09

electrochemical impedance of the prepared cells with the Pd- and $Cu_{0.5}Pd_{0.5}$-impregnated BZCYYb anodes was measured under the condition of open circuit in dry H_2 and CH_4, respectively, at temperatures 650 and 750 °C. With the ohmic resistance subtracted, the typical impedance spectra (measured at 750 °C) are shown in Fig. 6. The spectra are featured by two frequency dependent arcs, indicating the fuel oxidation reaction in the impregnated anodes was clearly separated into high and low frequency steps. The total polarization resistance R_P and the deconvoluted polarization resistances R_{p1} and R_{p2} were derived from the impedance spectra acquired at various temperatures, as listed in Table 1 together with those of the pure BZCYYb anodes.

In the case of H_2 fuel, it is noticed that with Pd or $Cu_{0.5}Pd_{0.5}$ impregnation into to the BZCYYb scaffold the overall R_P of the impregnated anodes for H_2 oxidation was reduced significantly in comparison with that of the BZCYYb anodes. For example, the R_P was 0.12 Ω cm² for the Pd- and $Cu_{0.5}Pd_{0.5}$-impregnated BZCYYb composite anodes at 750 °C, which is only around 1/5 of that of the pure BZCYYb anode at the same temperature. The same tendency was observed for the R_P measured at 650 °C. As a matter of fact, both the R_{p1} and R_{p2} were decreased simultaneously by the impregnation of the nano-sized catalyst particles into the BZCYYb anode due to the improved electronic conductivity of the composite anodes and the promoted electrode processes related to H_2 adsorption, dissociation and surface diffusion. However, the R_{p2} was decreased more considerably than the R_{p1}, which suggests that the nano-sized Pd or $Cu_{0.5}Pd_{0.5}$ particles is more effective in enhancing the electrode processes of H_2 adsorption, dissociation and diffusion than in providing the electronic paths in the anode for electron conduction. These phenomena are similar to what reported for the Pd-impregnated LCCM–GDC and Ni–GDC anodes [9,29]; and it is considered that Pd/PdO redox accelerates the low frequency electrode processes, because around 27% of the surface of impregnated Pd particles remains as PdO after high temperature H_2 reduction, and the presence of Cu further retards Pd reduction [9]. Also seen from Table 1, there is no significant difference in the impedance performance of the Pd- and $Cu_{0.5}Pd_{0.5}$-impregnated BZCYYb composite anodes for H_2 oxidation reaction, thus $Cu_{0.5}Pd_{0.5}$ impregnation is preferred for applications from the cost point of view.

With dry CH_4 as the fuel, the overall electrode polarization resistance R_P of the Pd- and $Cu_{0.5}Pd_{0.5}$-impregnated BZCYYb composite anodes was increased significantly, compared to that with H_2 as the fuel. However, no SEM evidence of carbon deposition was observed from the post-test samples, and the R_P increment became smaller with the increase of the measuring temperature. At 650 °C, the R_P of the Pd- and $Cu_{0.5}Pd_{0.5}$-impregnated BZCYYb anodes in dry CH_4 was 0.99 and 0.98 Ω cm², respectively, which is about 2.5 times of that in H_2. As the temperature was increased to 750 °C, the R_P for the both electrodes was decreased to 0.20 and 0.22 Ω cm², respectively, which is less than 2 times of that in H_2. Such electrochemical performance of the Pd- and $Cu_{0.5}Pd_{0.5}$-impregnated BZCYYb anodes in dry CH_4 is much more superior to that of the Pd-impregnated LCCM–GDC [9] and Ni–GDC [29] anodes. In order to further understand the electrode process of CH_4 oxidation in the BZCYYb anode with Pd or $Cu_{0.5}Pd_{0.5}$ impregnation, it is necessary to examine the deconvoluted polarization resistances R_{p1} and R_{p2}. From the data listed in Table 1, it is obvious that the oxidation reaction of CH_4 in the Pd- or $Cu_{0.5}Pd_{0.5}$-impregnated BZCYYb anodes is more likely dominated by the high frequency process than the low frequency one at the lower temperature 650 °C, and both high and low frequency processes become almost equally important at the higher temperature 750 °C. Further comparing the deconvoluted polarization resistances R_{p1} and R_{p2} in CH_4 and H_2, it is noticed that the R_{p1} was increased more significantly than the R_{p2}, which once again indicates that the impregnation of Pd or $Cu_{0.5}Pd_{0.5}$ is more likely to promote the low frequency electrode processes of CH_4 oxidation reaction as previously reported [9,29]. The oxidation of CH_4 may take an indirect pathway involving CH_4 cracking and electrochemical oxidation of the cracking products; therefore it

is required that the electrode is highly active for CH_4 cracking and electrochemical oxidation of the cracking products [30]. As well known, the BZCYYb is an active catalyst for reforming of hydrocarbon fuels such as CH_4 [12] and Pd shows high catalytic activity towards breaking the C–H bond of CH_4 [31]. Therefore, in the Pd- or $Cu_{0.5}Pd_{0.5}$-impregnated BZCYYb composite anodes, CH_4 could firstly be broken into C and H_2 at the dispersed Pd or $Cu_{0.5}Pd_{0.5}$ particles on the surface of the BZCYYb anode. Subsequently, H_2 produced by CH_4 decomposition is electrochemically oxidized to H_2O. The produced H_2O reacts with C to form CO and H_2. And then produced CO and H_2 are electrochemically oxidized to CO_2 and H_2O again without carbon deposition in the anode.

4. Conclusions

Based on the present study, the following conclusions can be made:

(1) The prepared BZCYYb possesses a cubic perovskite structure and is chemically compatible with the YSZ electrolyte at temperatures below 1000 °C in air. The electrochemical performance of the BZCYYb electrode characterized by the impedance spectra in H_2 is better than that of the LCCM–GDC, LCCM–YSZ and LSCM–YSZ composite anodes due to its higher catalytic activity and conductivity than those of the GDC, YSZ or LCCM phase in the composites electrode.

(2) Pd or $Cu_{0.5}Pd_{0.5}$ impregnation into the BZCYYb scaffold decreases the polarization resistance of the electrode R_P for H_2 oxidation by simultaneously decreasing the low- and high-frequency polarization resistances R_{p1} and R_{p2}; and the impregnated Pd or $Cu_{0.5}Pd_{0.5}$ particles are more effective in enhancing the low frequency electrode process that relate to H_2 adsorption, dissociation and diffusion than in providing the electronic paths in the anode for electron conduction.

(3) The electrode polarization of the Pd- or $Cu_{0.5}Pd_{0.5}$-impregnated BZCYYb anode in dry CH_4 is higher than that in H_2. It appears that the oxidation of CH_4 is more likely dominated by the high frequency process than the low frequency one at lower temperatures; and both high and low frequency processes almost equally contribute to the overall polarization at the higher temperatures.

(4) Pd and $Cu_{0.5}Pd_{0.5}$ impregnation are equivalently effective in enhancing the electrochemical performance of the BZCYYb anode in both H_2 and CH_4 atmospheres. And $Cu_{0.5}Pd_{0.5}$ is considered more appropriate as the impregnated species from the cost point of view.

Acknowledgements

This research was financially supported by the National Natural Science Foundation of China (U1134001) and the National "863" Project of China (2011AA050702). SEM and XRD characterizations were assisted by the Analytical and Testing Center of Huazhong University of Science and Technology.

References

[1] S.C. Singhal, Solid State Ionics 135 (2000) 305–313.
[2] A. Atkinson, S. Barnett, R.J. Gorte, J.T.S. Irvine, A.J. Mcevoy, M. Mogensen, S.C. Singhal, J. Vohs, Nat. Mater. 3 (2004) 17–27.
[3] S. McIntosh, R.J. Gorte, Chem. Rev. 104 (2004) 4845–4865.
[4] S.P. Jiang, S.H. Chan, J. Mater. Sci. 39 (2004) 4405–4439.
[5] S.D. Park, J.M. Vohs, R.J. Gorte, Nature 404 (2000) 265–267.
[6] E.P. Murray, T. Tsai, S.A. Barnett, Nature 400 (1999) 649–651.
[7] S.P. Jiang, X.J. Chen, S.H. Chan, J.T. Kwok, K.A. Khor, Solid State Ionics 177 (2006) 149–157.
[8] S.W. Tao, J.T.S. Irvine, Nat. Mater. 2 (2003) 320–323.
[9] A. Babaei, L. Zhang, S.L. Tan, S.P. Jiang, Solid State Ionics 181 (2010) 1221–1228.
[10] Y.H. Huang, R.I. Dass, Z.L. Xing, J.B. Goodenough, Science 312 (2006) 254–257.
[11] C.D. Zuo, S.W. Zha, M.L. Liu, M. Hatano, M. Uchiyama, Adv. Mater. 18 (2006) 3318–3320.
[12] L. Yang, S.Z. Wang, K. Blinn, M.F. Liu, Z. Liu, Z. Cheng, M.L. Liu, Science 326 (2009) 126–129.
[13] J.M. Vohs, R.J. Gorte, Adv. Mater. 21 (2009) 943–956.
[14] Z.Y. Jiang, C.R. Xia, F.L. Chen, Electrochim. Acta 55 (2010) 3595–3605.
[15] J. Chen, F.L. Liang, L.N. Liu, S.P. Jiang, B. Chi, J. Pu, J. Li, J. Power Sources 183 (2008) 586–589.
[16] J. Chen, F.L. Liang, D. Yan, B. Chi, J. Pu, S.P. Jiang, J. Li, J. Power Sources 195 (2010) 5201–5205.
[17] S.P. Jiang, F.L. Liang, J. Chen, F.Z. Wang, B. Chi, J. Pu, J. Li, Fuel Cells 9 (2009) 636–642.
[18] F.L. Liang, W. Zhou, B. Chi, J. Pu, S.P. Jiang, J. Li, Int. J. Hydrogen Energy 36 (2011) 7670–7676.
[19] F.L. Liang, J. Chen, J.A. Pu, B. Chi, S.P. Jiang, J. Li, J. Power Sources 196 (2011) 153–158.
[20] Z.H. Bi, J.H. Zhu, J. Power Sources 195 (2010) 3097–3104.
[21] S.P. Jiang, J. Chen, F.L. Liang, B. Chi, J. Pu, L. Jian, J. Power Sources 194 (2009) 275–280.
[22] S.P. Jiang, F.L. Liang, J. Chen, B. Chi, J. Pu, L. Jian, Electrochem. Commun. 11 (2009) 1048–1051.
[23] F.L. Liang, J. Chen, S.P. Jiang, B. Chi, J. Pu, L. Jian, Electrochem. Solid State Lett. 11 (2008) B213–B216.
[24] S. An, C. Lu, W.L. Worrell, R.J. Gorte, J.M. Vohs, Solid State Ionics 175 (2004) 135–138.
[25] L. Yang, C.D. Zuo, S.Z. Wang, Z. Cheng, M.L. Liu, Adv. Mater. 20 (2008) 3280-+.
[26] H.P. Ding, X.J. Xue, J. Power Sources 195 (2010) 7038–7041.
[27] Y.M. Choi, M.C. Lin, M.L. Liu, J. Power Sources 195 (2010) 1441–1445.
[28] S.P. Jiang, L. Zhang, X.B. Chen, H.Q. He, Y. Xiang, Solid State Ionics 180 (2009) 1076–1082.
[29] A. Babaei, S.P. Jiang, J. Li, J. Electrochem. Soc. 156 (2009) B1022–B1029.
[30] M. Mogensen, K. Kammer, Annu. Rev. Mater. Res. 33 (2003) 321–331.
[31] H. Uchida, S. Suzuki, M. Watanabe, Electrochem. Solid State Lett. 6 (2003) A174–A177.